ACS APPLIED POLYMER MATERIALS

Article

Cite This: ACS Appl. Polym. Mater. 2019, 1, 701−713

pubs.acs.org/acsapm

Multiple Physical Cross-Linker Strategy To Achieve Mechanically Tough and Reversible Properties of Double-Network Hydrogels in Bulk and on Surfaces

Yanxian Zhang,[†,⊥,#] Baiping Ren,[⊥,#] Shaowen Xie,[†,⊥] Yongqing Cai,[⊥] Ting Wang,[‡,⊥] Zhangqi Feng,[§,⊥] Jianxin Tang,[†] Qiang Chen,[∥] Jianxiong Xu,[†] Lijian Xu,[*,†] and Jie Zheng[*,⊥]

[†]Hunan Key Laboratory of Biomedical Nanomaterials and Devices College of Life Science and Chemistry, Hunan University of Technology, Zhuzhou 412007, China

[‡]State Key Laboratory of Bioelectronics Southeast University, Nanjing 210096, China

[§]School of Chemical Engineering, Nanjing University of Science and Technology, Nanjing 210094, China

[∥]School of Materials Science and Engineering, Henan Polytechnic University, Jiaozuo 454003, China

[⊥]Department of Chemical & Biomolecular Engineering, The University of Akron, Akron, Ohio 44325, United States

Supporting Information

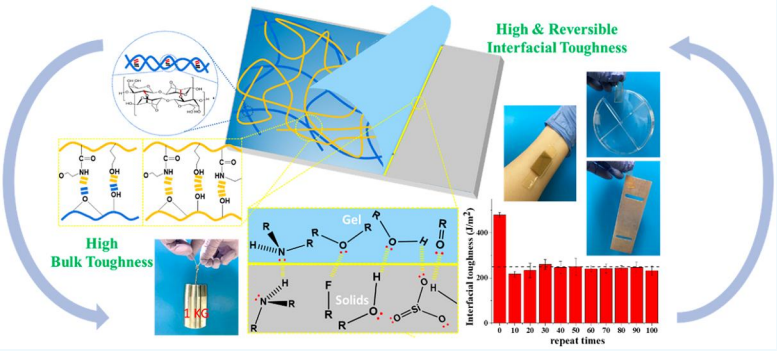

ABSTRACT: Development of tough and adhesive hydrogels is critical for different applications, including wound dressing, soft robotics, and wearable devices. However, achieving strong and reversible adhesion between hydrogels and surfaces have proved to be a great challenge, because strong adhesion and reversible adhesion are the two highly desirable but opposite properties of hydrogel adhesives. Existing hydrogel adhesives possess either one-time, irreversible, strong adhesion or reversible weak adhesion on diverse surfaces. Herein, we developed a fully physically cross-linked double-network (DN) hydrogel of Agar/pAAEE (N-poly(acryloylaminoethoxyethanol)) with both high bulk mechanical properties and strong reversible surface adhesion. Synergetic cooperation of high-density hydrogen bonds within both networks enables to simultaneously promote mechanical properties (tensile stress of 1.84 MPa, tensile strain of 2.5 mm/mm, elastic modulus of 1.85 MPa, and tearing energies of 1612 J/m^2) and fast mechanical self-recovery (stiffness/toughness recovery of 79%/60% in 5 min and 90%/91% in 30 min at 80 °C). In parallel to high mechanical properties in bulk, Agar/pAAEE DN hydrogels can not only virtually adhere to many untreated solid and soft surfaces (glasses, ceramics, aluminum, titanium, human skin) with high interfacial toughness up to ∼650 J/m^2 but also retain their strong and durable surface adhesion of 250 J/m^2 even after 100 times repeating adhesion-on/peeling off tests on glass substrate. Moreover, the hydrogels can also reversibly adhere on a human skin and detach from the skin without causing any damage, pain, and residue. High bulk toughness and strong surface adhesion of Agar/pAAEE gel are attributed to its double-network structure and dynamic/cooperative physical interactions within the networks and between network and surfaces. This free-standing, tough, and adhesive hydrogel could serve as promising materials for many adhesive-related applications.

KEYWORDS: *hydrogel, double network structure, mechanical properties, surface adhesion, interfacial toughness*

1. INTRODUCTION

Design of strong, reversible adhesive hydrogels remains an important but challenging problem for a wide range of applications such as biomedical devices,[1−3] wearable electronics,[4,5] soft robotics,[6,7] and biosensors.[8] In these applica-

Received: December 15, 2018
Accepted: February 26, 2019
Published: February 26, 2019

DOI: 10.1021/acsapm.8b00232
ACS Appl. Polym. Mater. 2019, 1, 701−713

tions, hydrogel adhesives are required not only to be tough enough to withstand high mechanical deformation but also to possess robust and reversible interfacial bonding on different surfaces. Ideally, hydrogel adhesives should be able to largely retain their adhesion after multiple peeling on-and-off actions from the surface, because reversible surface adhesion is highly desirable for certain applications (e.g., wearable devices and wound dressings). Unfortunately, most of hydrogel adhesives barely adhere to diverse surfaces as evidenced by their very low adhesion energy of 1−100 J/m^2,[9−13] easily lose adhesive capacity after multiple on-and-off peeling tests,[14,15] and lack self-recovery and self-healing functions to recover their adhesive and mechanical properties in a timely manner.[11,16,17] Such limits are mainly stemmed from the weak, brittle, and irreversible bonding (low fracture energies of ∼1−100 J/m^2, poor elastic modulus of ∼10 kPa, and limited self-healing properties)[14,18] both in bulk hydrogels and at hydrogel-surface interfaces, leading to difficulties in dissipating energy and reconstructing network structure. Weak adhesion is likely attributed to two main factors: weak mechanical properties of bulk hydrogel itself and weak interfacial bonding between hydrogel and surface.[19,20] Irreversible surface adhesion is often caused by a one-time peel-off action, so that the hydrogel−solid interface can not be regenerated back to its original adhesive state, presumably due to the permanent loss of major interfacial bonding. These limits prevent hydrogel adhesives from being used as wearable devices and gel-machine interfaces,[21−23] which require strong and reversible mechanical, adhesive, and self-healing properties. Currently, most of hydrogels still possess either property; that is, most of adhesive hydrogels are not tough hydrogels and vice versa.

To remedy the limits above, the design of a tough hydrogel with strong and reversible adhesion, in principle, should fulfill two criteria. On one hand, the bulk toughness of hydrogels needs to be significantly enhanced by introducing new network structures.[24] In this way, tough hydrogels could dissipate energy effectively when the interface is stressed. On the other hand, to improve interfacial toughness and its adhesive reversibility, the introduction of fully physically cross-linked networks, in line with surface modification,[20,25,26] supramolecular recognition,[27,28] and mechanical interlocking,[29,30] could offer a possibility to create strong but reversible binding sites at hydrogel−solid interfaces. However, challenges still remain, because bulk toughness versus interfacial toughness and toughness versus reversibility come from different origins.[19]

Recently, PAMPS/PAAm[29] and alginate/PAAm[31] double-network (DN) hydrogels were reported as tough and adhesive hydrogels. Both hydrogels can achieve high bulk toughness (1−5 MPa of tensile stress and fracture energy of ∼1000 J/m^2 for PAMPS/PAAm, ∼8000 J/m^2 for alginate/PAAm) and high interfacial toughness (1000 J/m^2 for PAMPS/PAAm,[29] 1000−1750 J/m^2 for alginate/PAAm[31]). But these strong adhesions require special treatment of substrates (either surface modification or porous structure) to realize high interfacial toughness; that is, PAMPS/PAAm hydrogels[29] achieved its high interfacial toughness by anchoring polymer chains inside porous solid substrates, while alginate/PAAm hydrogels achieve high interfacial toughness by chemically anchoring the long-chain polymers onto nonporous solid surfaces via the silane or 1-ethyl-3-(3-(dimethylamino)propyl) carbodiimide hydrochloride chemistry.[31] In addition, both PAMPS/PAAm and alginate/PAAm are chemically linked hydrogels, which lack self-recovery and reversible adhesion properties. Apart from hydrogel adhesives on solid and dry substrates, the chemically anchoring strategy can also be applied to the adhesion of hydrogels on wet or soft surfaces including human skin, pork heart, liver, artery, and cartilage. For instance, cyanoacrylate dispersed in 2,2,4-trimethylpentane, 1-octadecene, or paraffin oil[32] was used as a bonding agent to adhere hydrogels of PAAm, PAAm/alginate, PVA, and PHEMA on wet or soft surfaces (e.g., hydrogels, elastomers, leather), leading to strong interfacial toughness of ∼2000 J/m^2. However, the cytotoxicity of cyanoacrylate and organic solvent used in this system is a major concern for biorelated applications. To address this issue, new hydrogel adhesives, consisting of an adhesive layer containing polymer chains (e.g., chitosan, polyallylamine, polyethylenimine, collagen, gelatin) and a dissipative matrix (e.g., Alg, PAAm, Alg-PAAm), were developed as a general strategy to adhere on different soft tissues (skin, cartilage, heart, artery, liver) and soft hydrogels (Alg-PAAm, PAAm, PNIPAm, and PHEMA), with interfacial toughness of 100−1000 J/m^2 and without introducing any cell cytotoxicity.[33] In addition, several pH-triggered stitching polymers (e.g., chitosan, PAS, alginate, cellulose) were used as a stitch to connect two hydrogels together, producing a "sandwich-like" three-layer hydrogel.[34] The resultant sandwich-like hydrogels possessed high interfacial toughness of ∼2000 J/m^2. Overall, these chemical anchoring methods empower the strong adhesion of hydrogels to different surfaces (wet vs dry and solid vs soft), but these methods either require the pretreatment for substrates, complicated preparation procedures, or lack reversible surface adhesion capacity.

In contrast to the chemical anchoring, physical interaction-induced adhesive interfaces are more favorable due to the reversible and noninvasive nature to substrates. Inspired by mussels that could adhere to almost all soft and hard surfaces, hydrogels containing catechol groups have been widely used to realize the adhesion of gels on virtually all surfaces.[14,35−38] However, a proved drawback of catechol-induced adhesive interface is that it is easily subjected to oxidization, leading to the irreversible loss of surface adhesion. In addition, these hydrogels generally suffer from mechanical weakness and, thus, cannot meet the toughness and stretchability as required for practical applications.[12,39,40] Apart from the mussel-inspired adhesives, other biomolecules, for example, the nucleobases of adenine (A) and thymine (T), have also been used as adhesive groups for hydrogel adhesives due to the presence of a large amount of hydrogen bondings.[41] Beyond that, the creation of a certain micropattern of hexagonal facets on the charge balanced polyampholyte (PA) hydrogel enables to improve the interfacial toughness of PA gel on various surfaces, leading to reversible yet weak surface adhesion (<50 J/m^2) under water.[7] These physical hydrogel adhesives—as anchored by hydrogen bonds, metal complexation, and hydrophilic interactions—endow certain degrees of surface adhesion reversibility, but adhesion energy (i.e., interfacial toughness) of these hydrogels was too low to be used for wound dressing, soft robotics, or biomedical devices with reliable and reversible adhesion.

Different from these hydrogels, we recently designed a fully physically linked Agar (1st network)/poly(*N*-hydroxyethyl acrylamide) (pHEAA, second network) DN hydrogel, where both networks are physically cross-linked via hydrogen bonds.[42] Agar/pHEAA DN hydrogels exhibited superior mechanical strength/toughness and self-recovery property in

DOI: 10.1021/acsapm.8b00232
ACS Appl. Polym. Mater. 2019, 1, 701−713

bulk. More importantly, without any surface modification, Agar/pHEAA hydrogels can easily and strongly adhere to different nonporous solid surfaces including glass, titanium, aluminum, and ceramics, demonstrating the extremely high interfacial toughness of ~2000–7000 J/m^2, far beyond that of tendon/cartilage bonds and other adhesive hydrogels. However, because of its super strong surface adhesion, Agar/pHEAA hydrogel can not easily be peeled off from the substrates, thus lacking reversible surface adhesion. To overcome this limit, here we redesigned the second network by replacing pHEAA with poly(*N*-acryloylaminoethoxyethanol) (pAAEE) to produce a new fully physically linked Agar/pAAEE DN hydrogel. The first agar network is formed by the association of agar helical bundles via hydrogen bonds, while the second pAAEE network is also formed by hydrogen-bond association and chain entanglement, since AAEE monomer contains three hydrophilic groups, amide, ethylene glycol ($-CH_2CH_2-O-$), and hydroxyl group, where any two neighboring groups are separated by two carbon space length. Multiple hydrogen-bonding groups from both networks allow to construct highly cooperative physical networks, which help to realize mechanical reinforcement. Different from the amide and hydroxyl group in AAEE that serve as both hydrogen-bonding donors and acceptors, the ethylene glycol group only works as hydrogen-bonding acceptor, which would regulate the noncovalent interfacial bondings for achieving the modest and reversible adhesive properties to various surfaces that contain abundant oxygen/nitrogen atoms as hydrogen-bonding acceptors without any surface modification. As a result, Agar/pAAEE DN hydrogels demonstrated not only their high tensile strength (~1.84 MPa) and high fracture energy (~1600 J/m^2) in bulk but also their strong yet reversible surface adhesion on different substrates with the repeatable adhesion of ~250 J/m^2 up to 100 times peeling off-and-on tests. The reversible breaking and reforming of hydrogen bonds between hydrogel networks and between the networks and substrates accounts for the self-recovery and reversible adhesion properties of hydrogel adhesives. We hope that this new Agar/pAAEE hydrogel will provide new design strategy and knowledge for developing high-performance adhesive materials for diverse applications.

2. MATERIALS AND METHODS

2.1. Materials. Acryloyl chloride (97.0%), hydroquinone, 2-(2-aminoethoxy)ethanol (98%), ethanol (absolute 200 proof), isopropyl alcohol, chloroform, agar (microbiology grade, gel strength >800 g/cm^2 with melting point of 85–95 °C), 2-hydroxy-4′-(2-hydroxyethoxy)-2-methylpropiophenone (Irgacure 2959, 98%) were purchased from Sigma-Aldrich. Silica gel (0.036–0.071 mesh) was purchased from Alfa Aesar. Water was purified by a Millipore water purification system (18.2 MΩ·cm resistivity).

2.2. Synthesis of AAEE Monomer. The AAEE monomer was synthesized by the reaction of acryloyl chloride and 2-(2-aminoethoxy) ethanol as reported in our previous work.[43] Acryloyl chloride (4.53 g, 0.05 mol) dissolved in 100 mL of absolute ethanol was added into a three-necked flask, and the solution was cooled to −40 °C with isopropyl alcohol/dry ice bath. 2-(2-Aminoethoxy) ethanol was diluted with 100 mL of absolute ethanol, added into the flask dropwise. After it reacted at −40 °C for 2 h, the mixture was further stirred overnight at 2–4 °C. The crude product was concentrated and extracted into acetone after the precipitated salt was filtered out and was further purified by silica gel column. AAEE was stored with hydroquinone as stabilizer at 2–4 °C. The yield was 67%. ^{1}H NMR (300 Hz, D_2O): δ 6.10–6.26 (m, 2H), 5.68–5.71 (ddd, 1H), 3.55–3.67 (m, 6H), 3.40–3.43 (m, 2H). ^{13}C NMR (300H, D_2O): δ 168.89, 130.11, 127.95, 71.45, 68.08, 60.32, 38.41.

2.3. Agar/pAAEE DN Hydrogel Preparation. The fully physical cross-linked Agar/pAAEE DN hydrogels were synthesized using the one-pot heating–cooling-photopolymerization method as reported in our previous work.[44] Briefly, 50 mg/mL agar, 50 wt % AAEE, UV initiator (1 mol % of AAEE), and water were added into a tube and degassed with nitrogen. After they were gradually heated to 95 °C, all reactants dissolved in water and formed a transparent solution. The solution was then injected into a mold and cooled at room temperature to first form the physically cross-linked network (agar gel). Then, the remaining AAEE in the same pot was photopolymerized under UV light (wavelength: 365 nm, intensity: 8 W, UVP, CA) for 1 h. This procedure allowed the second fully physically cross-linked pAAEE network formed by interpenetrating through the already existing first agar network. After these simple heating–cooling-photopolymerization steps, gels were removed from the molds, sealed, and stored at 2–4 °C before any tests. Similarly, the agar single network (SN) hydrogels were prepared with heating–cooling method without photopolymerization steps, and the pAAEE SN hydrogels were synthesized with single photopolymerization process.

2.4. Mechanical Testing. *Tearing Test.* Trousers-shaped (40 mm in length, 20 mm in width, and 1 mm in thickness) sample was used in the tearing test with an initial notch of 20 mm. One arm of the sample was clamped and fixed, while the other arm was clamped and pulled upward at a velocity rate of 100 mm/min. The tearing energy is defined as the force required to tear per unit area and is estimated by $T = 2F_{ave}/\omega$,[45] where F_{ave} is the average force of peak values during steady-state tearing, and ω is the thickness of the specimen.

Tensile Test. The tensile tests were performed on a universal tester (Instron 3345, MA) equipped with a 500 N load cell at 100 mm/min crosshead speed. The gels were cut into dumbbell shape (ASTM-638-V) with a gauge length of 25 mm, a width of 3.18 mm, and a thickness of 1 mm. The tensile strain (ε) was the elongation of the sample (Δl) divided by its initial length (l_0) ($\varepsilon = \Delta l/l_0$). The tensile stress ($\sigma$) was the load force ($F$) divided by the original cross-sectional area (A_0) of the specimen ($\sigma = F/A_0$). For hysteresis tests, specimens were first stretched to a maximum strain of $\varepsilon = 1.5$ using the same tensile tester, then unloaded at the same rate of 100 mm/min. The loading–unloading cycles were repeated several times. And for recovery experiments, the specimens were sealed and stored at 80 °C or room temperature after first loading–unloading cycle. Then the specimens were cooled at room temperature before the tests. The fracture energy dissipated during each loading–unloading cycle (U_{hys}) was estimated by the area between the loading–unloading curves.

Compression Test. The compression test was performed with a 500 N load cell at 10 mm/min crosshead speed. The gels were synthesized in a 4 mm diameter cylindrical mold with a height of 3.5 mm. The samples were placed on the center of the test plate and compressed by the load cell. The maximum compression strength was determined by the force that applied to per cross-sectional area of the sample with 90% compression strain.

Lap-Shear Test. The lap-shear tests were also performed on the tensile tester. The hydrogels were prepared in sandwich-like mold with microscope glass slides (75 mm × 25 mm × 1 mm) on both sides and a 1 mm Teflon spacer. The resulting contact area between the hydrogel and the glass was 23 mm × 15 mm. Each side of glass was clamped, and one of the clamps was pulled up at constant crosshead speed, while the other was fixed. The maximum adhesive strength was determined by the force that completely separated the overlapped glass plates divided by the contact area.

Peeling Test. The interfacial toughness between the hydrogel and the substrates were measured using 90° peeling tests with a 90° fixture (Mecmesin, ACC008-208) on the mechanical tester. Hydrogels adhered on various surfaces were tested with a standard 90° peeling test at the crosshead speed of 50 mm/min. A Scotch duct tape (3M) was adhered on the side of hydrogel as a stiff backing for peeling test. The interfacial toughness was estimated by the average force (F_{ave}) in

DOI: 10.1021/acsapm.8b00232
ACS Appl. Polym. Mater. 2019, 1, 701–713

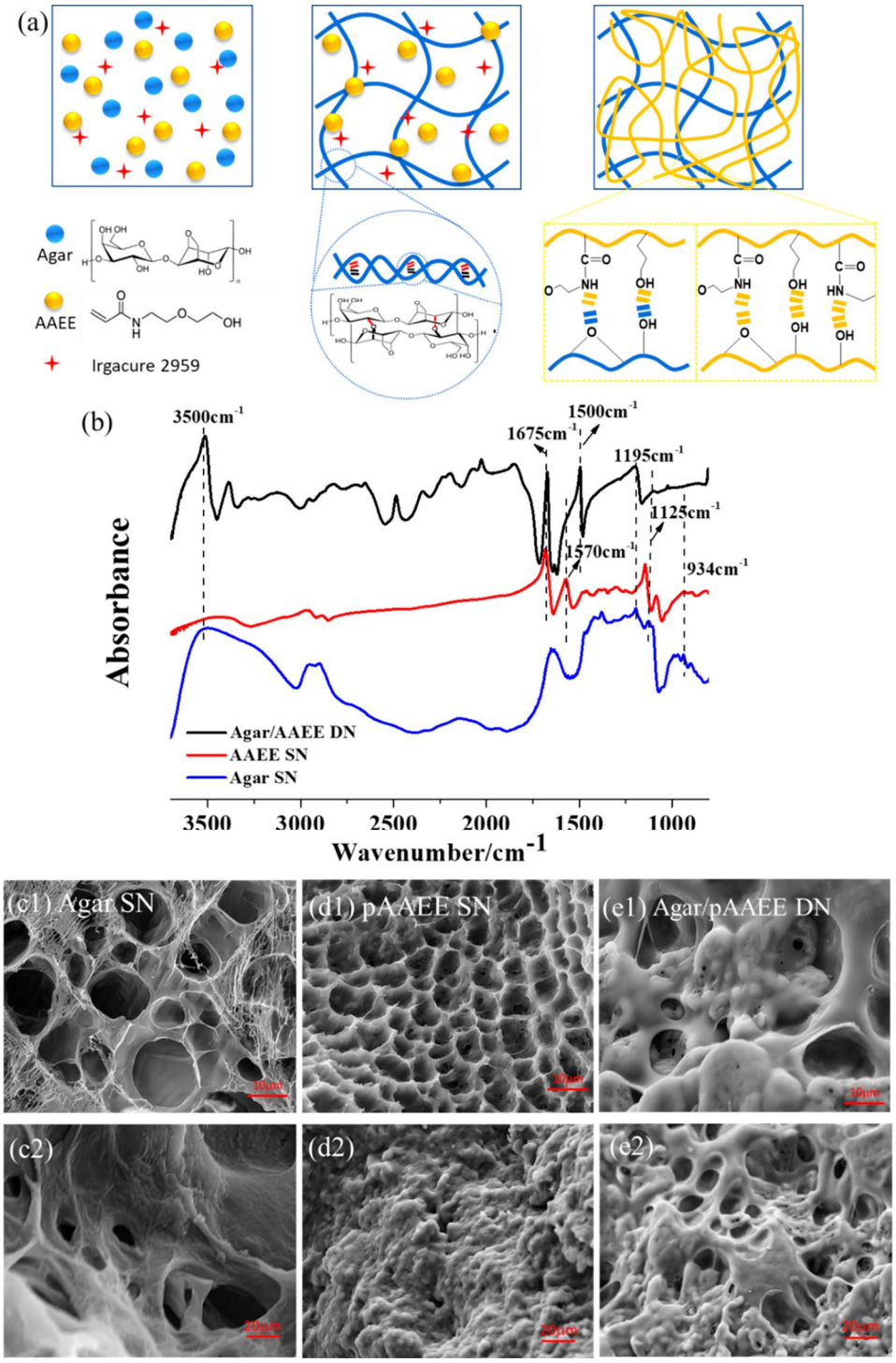

Figure 1. (a) Synthesis of Agar/pAAEE DN hydrogels. (b) FTIR spectra, SEM cross-sectional (c1, d1, e1) and side surface (c2, d2, e2) images of Agar SN, pAAEE SN, and Agar/pAAEE DN hydrogel.

the steady-state region during the peeling process per width (w) of the hydrogel ($g = F_{ave}/w$).

3. RESULTS AND DISCUSSION

3.1. Synthesis and Characterization of Agar/pAAEE DN Gels. As a family member of the acrylamide-based monomers, AAEE was first reported and used for electrophoresis application[46] due to its high hydrophilicity and hydrolytic stability. In this work, AAEE monomer was synthesized by replacing the end −Cl group of acryloyl chloride with 2-(2-aminoethoxy) ethanol and confirmed by $^{1}H/^{13}C$ NMR spectra, as shown in Figures S1 & S2. AAEE monomer contains three hydrophilic groups: an amide group (−CONH−), ethylene glycol group (−CH_2CH_2−O−), and a hydroxyl group (−OH) at the end. Given the abundant hydrophilic groups, AAEE monomer is a promising candidate

DOI: 10.1021/acsapm.8b00232
ACS Appl. Polym. Mater. 2019, 1, 701−713

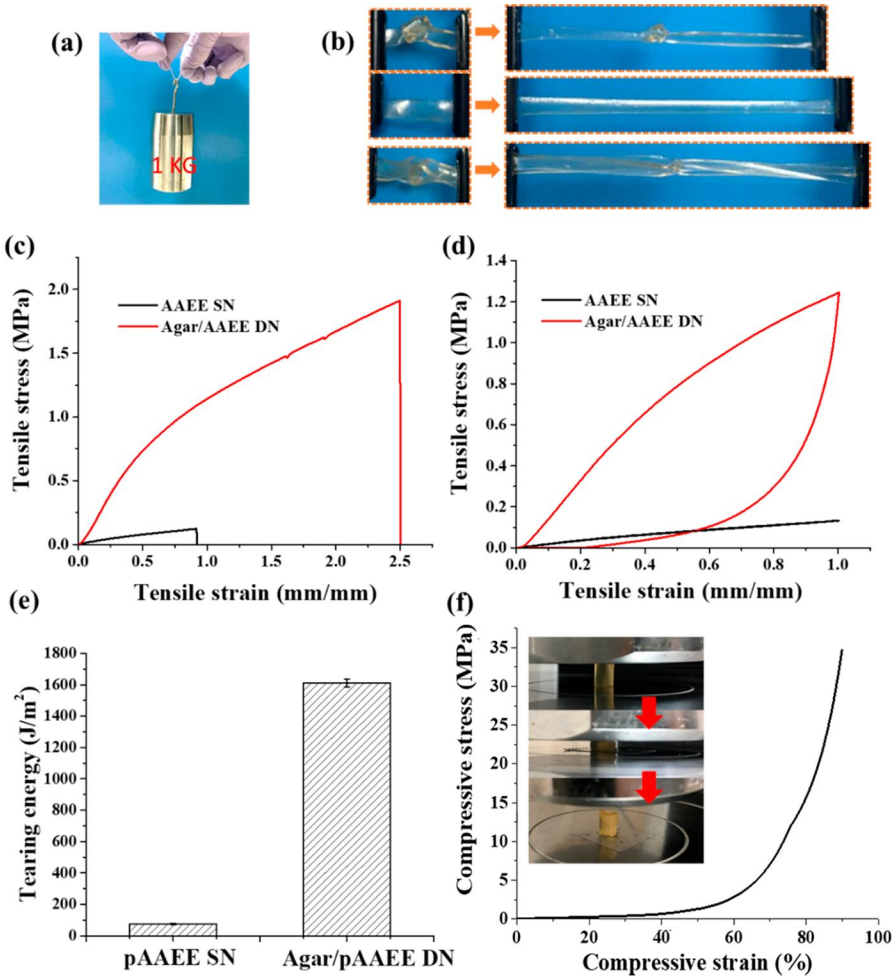

Figure 2. Visual inspection of mechanical properties of as-prepared Agar/pAAEE DN hydrogels by (a) weight lifting and (b) knotted, original, and crossover stretching. Comparison of mechanical properties of as-prepared pAAEE SN and Agar/pAAEE DN hydrogels by (c) tensile, (d) loading–unloading, (e) tearing, and (f) compression tests.

to form a fully physically cross-linked network via hydrogen bonds, in which the dynamic and reversible hydrogen-bonded network offers a possibility to introduce self-recovery property and reversible surface adhesion.

Upon synthesis of AAEE, Agar/pAAEE hydrogel was prepared by a facile one-pot heating–cooling-photopolymerization method as reported in our previous works.[19,47,48] Briefly, as shown in Figure 1a, all reagents (without any chemical cross-linkers), including agar, AAEE, and UV initiator, were dissolved in water and heated to 95 °C for 10 min. Then, the solution was gradually cooled to room temperature, and the first agar network was formed via a thermo-induced sol–gel transition at the same time. During this sol–gel gelation process, agar molecules underwent the conformational change from random coils to α-helix, followed by the aggregation of α-helical agars into the helical bundles via hydrogen bonds to form the first physical network. Next, UV light (λ = 365 nm, intensity = 8 W) was introduced to photopolymerize AAEE monomers to form the second physical network, interpenetrating with but independent of the first agar network. For comparison, similar heating–cooling and photopolymerization methods were used separately to prepare the single-network (SN) agar hydrogel and pAAEE hydrogel, respectively.

FTIR spectroscopy in Figure 1b was used to characterize the chemical structure of Agar/pAAEE DN hydrogels as compared to Agar SN and pAAEE SN hydrogels. Agar SN hydrogel displayed several characteristic adsorption peaks of −OH stretching at 3500 cm^{-1}, glycosidic bonding at 1195 and 1125 cm^{-1}, and C−O−C bridge at 934 cm^{-1}.[49] pAAEE SN hydrogel had strong characteristic amide absorption peaks at 1675 cm^{-1} (amide-I, C=O stretching), 1570 cm^{-1} (amide-II, NH bending), and 934 cm^{-1} (C−O−C bridge), respectively. Consistently, all characteristic adsorption peaks appearing in Agar and pAAEE SN hydrogels were also observed in Agar/pAAEE DN hydrogel. For instance, the increase of −OH stretching intensity implies abundant hydrogen bonds being formed in the double network. The characteristic absorption peak of amide II (NH bending) at 1570 cm^{-1} was transferred to 1500 cm^{-1}, indicating the interaction between Agar and -NH groups of AAEE. In parallel, representative scanning electron microscopy (SEM) images were further used to characterize the interior network morphologies of three freeze-dried hydrogels. Agar SN hydrogels presented a much larger and loose cross-sectional structure with ~10–20 μm pore size (Figure 1**c1**) and nonuniform sideview structure (Figure 1**c2**), while pAAEE SN hydrogels presented a uniform spongelike structure at the cross-section with average pore size of ~5 μm

DOI: 10.1021/acsapm.8b00232
ACS Appl. Polym. Mater. 2019, 1, 701–713

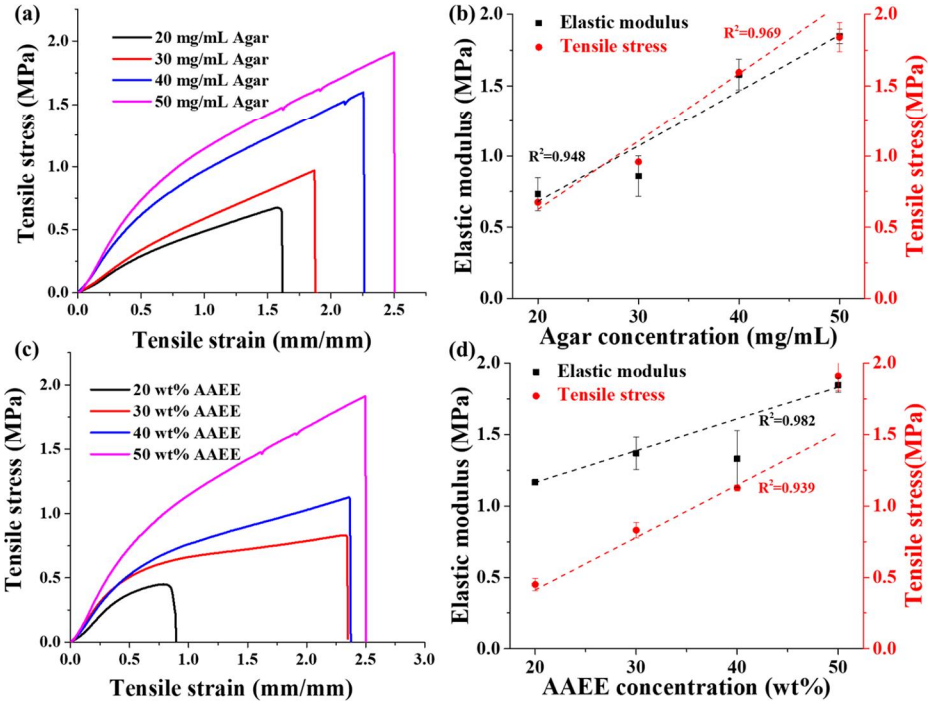

Figure 3. Mechanical properties (stress–strain curves) and the corresponding linear fitting for tensile stress and elastic modulus of as-prepared Agar/pAAEE DN hydrogels as a function of (a, b) agar concentrations and (c, d) AAEE concentrations.

(Figure 1**d1**) and a spherical stacking structure from a side viewpoint (Figure 1**d2**). Upon sequential polymerization of the two networks, two polymers tended to interpenetrate and fill the interior pores of hydrogel networks, whose porosity and morphology were significantly different from that of either SN hydrogel (Figure 1e). This proves that the two networks are indeed embedded on the surface of the pores to form the densely interpenetrating networks.

3.2. Mechanical Properties of Agar/pAAEE DN Gels. For a first proof-of-concept, an as-prepared Agar/pAAEE DN hydrogel exhibited strong mechanical properties, which hold a large weight of 1 kg up to almost 1000 times of its own weight (Figure 2a) and withstand original stretching, knotted stretching, and crossover stretching up to 4 times of its original length (Figure 2b). Furthermore, we provided a side-by-side comparison of mechanical properties between Agar/pAAEE DN gels and agar or pAAEE SN gels to demonstrate the double-network structural enhancement effect using tensile, cyclic loading–unloading, tearing, and compression tests. pAAEE SN hydrogel was very fragile with extremely low tensile stress of 0.123 MPa and tensile strain of 0.91 mm/mm, while Agar SN hydrogel was too weak to be tested. But, when the two weak networks were interpenetrated with each other, the resultant Agar/pAAEE DN gel significantly improved its tensile stress to ~1.84 MPa and tensile strain to ~2.5 mm/mm (Figure 2c). The cyclic loading–unloading test also showed that Agar/pAAEE DN gel presented a very large hysteresis loop corresponding to a notable dissipated energy (U_{hys} = 549.5 kJ/m^3), in sharp contrast to the extremely small hysteresis loop of the pAAEE SN gel with almost neglectable energy dissipation (U_{hys} = 0.001 kJ/m^3; Figure 2d). As indicated from the energy dissipation capacity, Figure 2e confirmed that Agar/pAAEE DN gel exhibited very high tearing energy of ~1612 J/m^2, which was 20 times higher than that of pAAEE SN gel (~76 J/m^2). Such high toughness of fully physical Agar/pAAEE DN gel is comparable to that of the chemically cross-linked DN hydrogels (~100–1000 J/m^2)[50−52] and cartilages (~1000 J/m^2).[43] Compression test revealed that the DN gel can achieve a very high compressive stress of ~34.7 MPa at 90% stain at a compression rate of 10 mm/min (Figure 2f). But, as a compression rate increased to 100 mm/min, compressive stress decreased to 25.0 MPa at the same compressive strain of 90%. Considering that all SN and DN hydrogels exclusively contain physical networks without any chemical cross-linkers, the two hydrophilic networks work synergistically to form a massive hydrogen-bonding network. The second AAEE polymer network is highly resilient and stretchable, creating a large process zone, while the first agar network with its unique helix bundle chains is not stretchable but highly energy dissipative with large mechanical hysteresis, thus dissipating energy within the process zone. Taken together, Agar/pAAEE DN hydrogels dissipate energy much more efficiently than pAAEE SN gel upon deformation, leading to the enhanced mechanical strength and toughness.

Intuitively, the stiffness and toughness of Agar/pAAEE DN gels can be changed by varying the concentration of the two networks. To better understand the DN-induced mechanical reinforcement mechanism, we prepared Agar/pAAEE DN gels under widely varied fabrication conditions and performed a series of tensile tests to examine the effects of Agar and AAEE concentrations on the mechanical properties of Agar/pAAEE DN gels, and results were summarized in Figure 3 and Table S1. It can be seen in Figure 3a,b that, as the concentration of agar increased from 20 to 50 mg/L at a fixed AAEE concentration of 50 wt %, Agar/pAAEE DN gels monotonically increased tensile stress from 0.67 to 1.84 MPa, elastic modulus from 0.73 to 1.85 MPa, and fracture strains from 1.6 to 2.5 mm/mm, respectively. Similarly, in the case of AAEE effect (Figure 3c,d), both tensile stress and elastic modulus of Agar/pAAEE gels increased from 0.45 to 1.84 MPa and from

DOI: 10.1021/acsapm.8b00232
ACS Appl. Polym. Mater. 2019, 1, 701−713

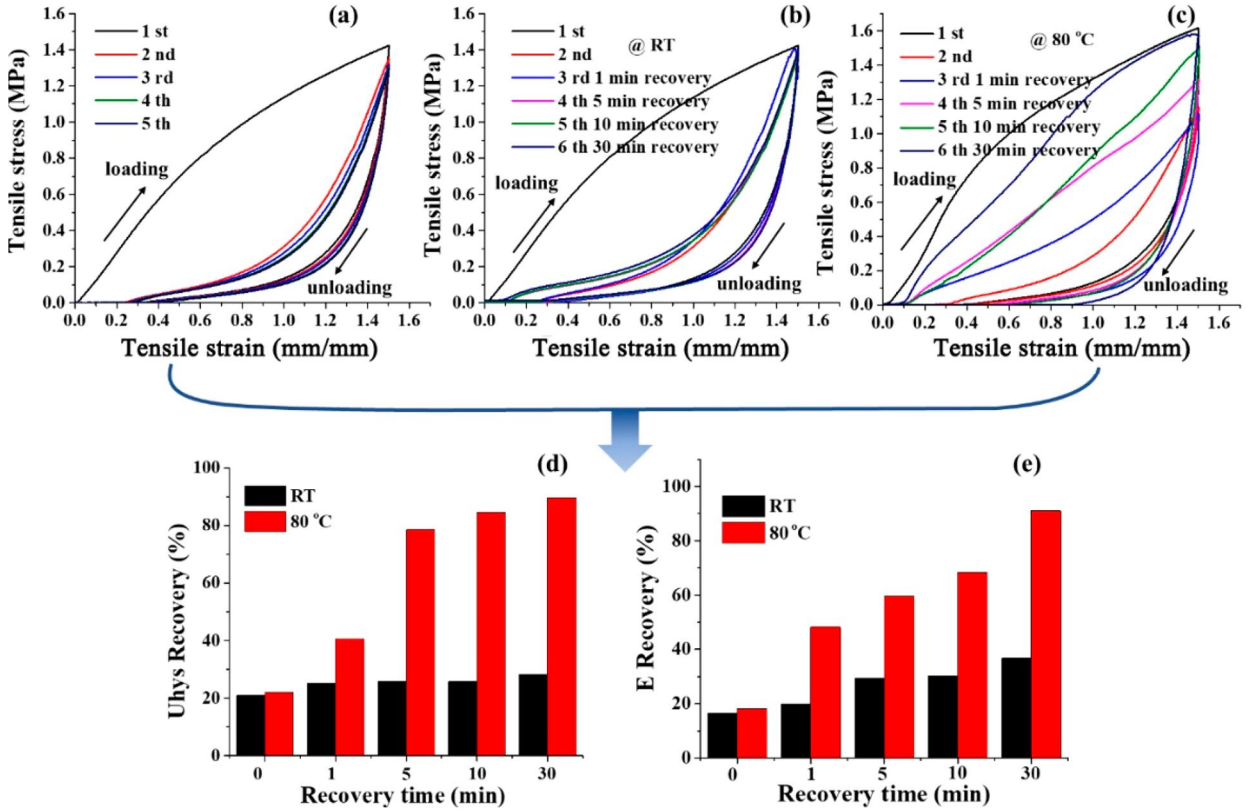

Figure 4. Mechanical self-recovery of Agar/pAAEE DN hydrogels using hysteresis loading–unloading tests, as indicated by hysteresis loops of Agar/pAAEE DN hydrogels (a) without recovery time at room temperature, (b) with different resting times at room temperature, and (c) with different resting times at elevated temperature of 80 °C, as well as (d) toughness (energy loss) and (e) stiffness (elastic modulus) recovery of Agar/pAAEE DN gels extracted from (a–c) curves.

1.17 to 1.85 MPa, respectively, as AAEE concentration increased from 20 to 50 wt % at a fixed agar concentration of 50 mg/L. However, when AAEE concentration was higher than 30 wt %, fracture strains retained almost unchanged at ~2.5 mm/mm. Collective mechanical data reveal that Agar/pAAEE DN gels achieve the best mechanical properties of the combinations we tested (tensile stress of ~1.84 MPa; elastic modulus of ~1.85 MPa; and fracture stain of ~2.5 mm/mm) at Agar of 50 mg/mL and AAEE of 50 wt %. Note that our previous works in Agar/PAM, Agar/HPAAM, Agar/HEAA, BSA/PAAm, and Agar/PAMAAc-Fe_{3+} hydrogels have shown that the further increase of the concentrations of either network component does not necessarily result in the higher mechanical properties. For instance, the agar network is rigid and brittle; thus, the increase of agar concentrations could increase elastic modulus and fracture stress but decrease fracture strain. The second pAAEE network is softer and more ductile, and the increase of pAAEE could increase tensile stain at the expense of mechanical stress and modulus. So, a delicate balance of the two network components and concentrations is equally important for achieving the best mechanical properties for any DN hydrogel. More importantly, both tensile stress and elastic modulus increased almost linearly as agar or AAEE concentrations, with R^2 values of 0.94–0.98 (Figure 3b,d). This indicates that both stiffness and toughness of Agar/pAAEE DN gels can be simultaneously enhanced by tuning agar or AAEE concentrations. This behavior is different from that of conventional chemically linked hydrogels, in which stiffness and toughness are usually inversely related to each other. For chemically linked hydrogels, high stiffness leads to the sufficient elastic energy accumulation to precipitate failure by chain scission, which results in low toughness. Unlike chemically cross-linked hydrogels that fracture by chain scission, the fracture of our fully physically linked Agar/pAAEE hydrogels is determined by the viscous pulling-out of chains from both networks by disrupting noncovalent interactions, consistent with several studies of physically linked gels.[53,54] Therefore, the increase of agar concentration would require the higher strain to complete the helix–coil transition and the chain pull-out process, both of which will dissipate energy in a more efficient way for improving hydrogel toughness. In parallel, as the increase of AAEE concentration, the physically noncovalent interactions within the pAAEE network and between the two networks are both enhanced, leading to the higher strain and energy to unzip and slide polymer chains in the networks. In both scenarios, Agar/pAAEE DN hydrogels exhibit a positive correlation of agar and AAEE concentrations with both stiffness and toughness.

Furthermore, cyclic loading–unloading experiments were performed to evaluate the energy dissipation and self-recovery of Agar/pAAEE DN gels in response to different resting times and temperatures. As a control in Figure 4a, Agar/pAAEE DN gels were tested by five loading–unloading cycles at a strain of 1.5 and room temperature without any resting time between cycles. In the first loading–unloading cycle, Agar/pAAEE DN gel presented a large hysteresis loop with large dissipated energy (~1.03 MJ/m^3), as expected for physically cross-linked double networks.[55,56] But in the immediately following

DOI: 10.1021/acsapm.8b00232
ACS Appl. Polym. Mater. 2019, 1, 701–713

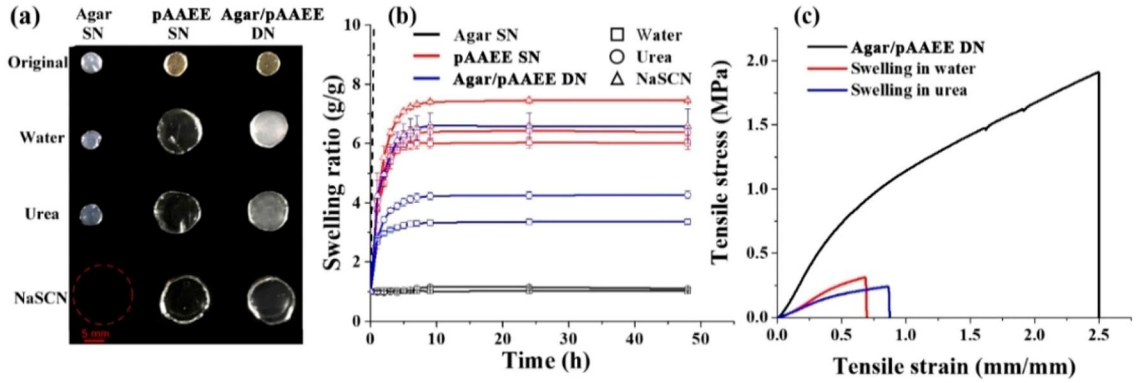

Figure 5. Swelling behaviors of Agar SN, pAAEE SN, and Agar/pAAEE DN hydrogels in different soaking solutions of water, urea, and NaSCN, including (a) side-by-side swelling image comparison between as-prepared and swollen gels; (b) swelling ratios, and (c) tensile properties.

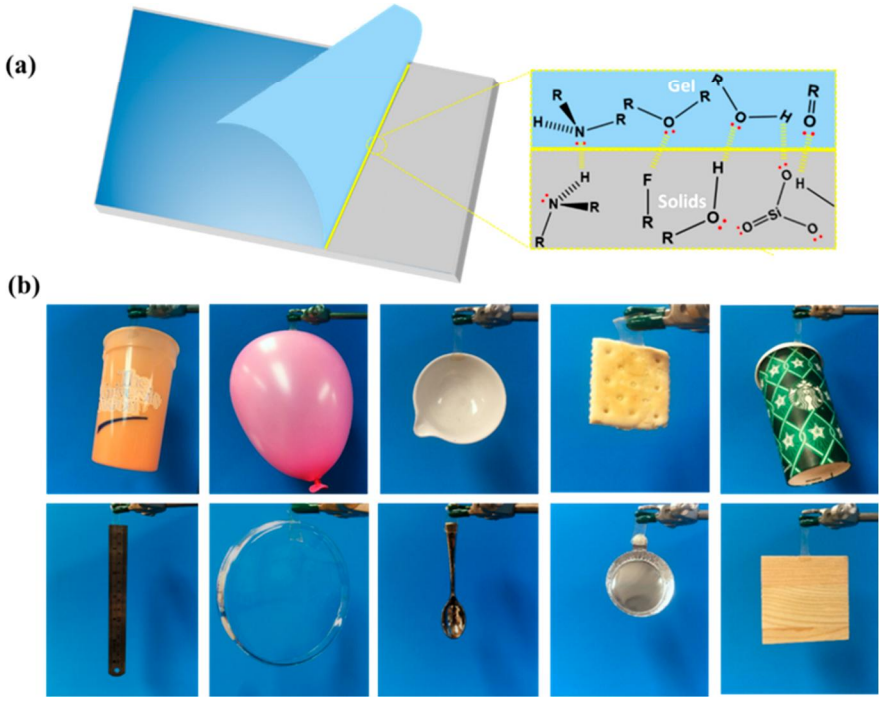

Figure 6. (a) Schematic of interfacial interactions between Agar/pAAEE DN hydrogel and a solid surface. (b) Agar/pAAEE DN hydrogel can directly adhere on various solid surfaces without any surface modification.

second–fifth cycles, the gel displayed small hysteresis loops ($U_{hys} \approx 0.26$ MJ/m^3), all similar to each other due to the softening occurrence from the ruptured physical bonds.[57,58] This indicates that the fractured networks can not be recovered immediately without any resting at room temperature. On the other hand, because of the physical nature of the both networks, we further examined both elastic modulus-based (stiffness) self-recovery and dissipated energy-based (toughness) self-recovery of Agar/pAAEE DN gels in response to resting time and temperature after the first loading–unloading. In Figure 4b, without any external stimuli, the DN gels recovered their toughness/stiffness by 25.2%/19.9%, 25.8%/29.4%, and 28.3%/36.8% after 1, 5, and 30 min resting at room temperature, respectively. Moreover, considering the thermo-induced sol–gel transition of the agar network, the self-recovery of Agar/pAAEE DN gels could be largely improved at elevated temperatures (>80 °C) due to the additional recovery from the agar network. As shown in Figure 4c–e, after the gels were incubated at 80 °C (higher than sol temperature of agar), the toughness/stiffness recovery rates were largely increased to 40%/48%, 79%/60%, 85%/68%, and 90%/91% after 1, 5, 10, 30 min of heating time, respectively.

Since Agar/pAAEE DN hydrogels are fully physically cross-linked by hydrogen bonds, the cooperative hydrogen bonds are expected to play a vital role in improving mechanical and self-recovery properties. To test this hypothesis, we introduced the two well-known hydrogen-bond breaking reagents (i.e., urea and NaSCN, where NaSCN is more destructive for hydrogen bonds than urea) to treat Agar/pAAEE DN hydrogel, followed by the study of how urea and NaSCN affect the network structure, interaction, and mechanical properties of physical hydrogels. When Agar/pAAEE DN, Agar SN, and AAEE SN hydrogels were immersed into water, 5 M urea, or 5 M NaSCN solution at room temperature for 48 h, we compared the swelling behaviors and mechanical properties of these hydrogels in aqueous, urea, and NaSCN solutions. Visual

DOI: 10.1021/acsapm.8b00232
ACS Appl. Polym. Mater. 2019, 1, 701–713

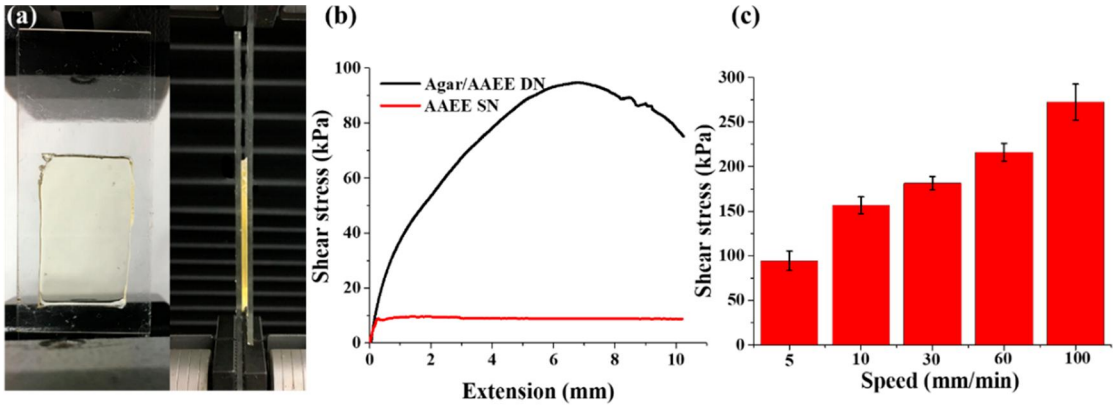

Figure 7. (a) Experimental setup for lap shear tests on AAEE SN and Agar/pAAEE DN hydrogels adhered between the two glass slides, with the adhesion results of (b) shear stress-extension profiles and (c) shear stress as a function of shear speed.

inspection in Figure 5a showed that swollen Agar/pAAEE DN hydrogels remained almost unchanged in volume and showed opaque white color in water and urea, but the gel immersed in NaSCN solution became transparent. For comparison, agar SN gels barely swell in water and urea and showed initial opaque white, but they were dissolved in NaSCN immediately and completely. All pAAEE SN gels were highly swollen and became transparent in water, urea, and NaSCN solutions. Quantitively, Figure 5b shows the swelling kinetics of three hydrogels in water, urea, and NaSCN solutions. It can be seen that all hydrogels (except for Agar SN hydrogel) in different solutions tended to swell as time went by and reached to equilibrium swelling after ~10 h. For a given hydrogel, different solvents induced different degrees of hydrogel swelling, showing a consistent but increased swelling order of water < urea < NaSCN. This phenomenon became even more pronounced for Agar SN gels in NaSCN solution that completely dissolved the gels. As a result, the equilibrium swelling ratio of Agar/pAAEE DN hydrogels was ~3.2 in water, ~4.2 in urea, and ~6.5 in NaSCN, which were smaller than that of AAEE SN hydrogels of ~6 in water, ~6.5 in urea, and ~7.5 in NaSCN. Thus, the introduction of DN structure enables to greatly suppress the expansion of gel networks. As expected, the swollen transparent Agar/pAAEE hydrogel became mechanically weak, and its tensile stress/strain were significantly reduced to 0.3 MPa/0.7 in water and 0.2 MPa/0.9 in urea, respectively (Figure 5c), due to the breaking of hydrogen bonds and lower polymer volume fraction. The swollen DN gels in NaSCN were too weak to be measured by tensile test. Thus, the contribution of hydrogen bonding to the high mechanical strength of DN hydrogels was proven by the fact that the strength decreased significantly after swelling in urea or NaSCN solution.

3.3. Interfacial Toughness (i.e., Surface Adhesion) of Agar/pAAEE DN Gels. Adhesive hydrogels on different soft or hard surfaces (muscle tissues, plastics, rubbers, glasses, metals, ceramics, carnelians, and woods) always have great potential for many applications, such as electronic skin, wound dressing, and wearable devices. It is generally accepted that strong interfacial toughness (i.e., high adhesion strength) of hydrogels on surfaces depends on the mechanical strength of hydrogels itself and intermolecular interactions between hydrogels and surfaces. Since Agar/pAAEE hydrogels have demonstrated their high toughness of 1612 J/m^2 and strength of 1.84 MPa in bulk, it is important to enhance hydrogel–surface interactions. On the basis of the molecular structure of Agar/pAAEE hydrogels, the presence of abundant hydrophilic groups of hydroxyl group (−OH), O−glycosidic bonds in agar and hydroxyl group (−OH), amide group (−CONH−), and ethylene glycol (EG, $-CH_2CH_2-O-$) in pAAEE would provide more physical interactions via hydrogen bonding, metal complexation, and van deer Waal interactions for surface adhesion on different solid surfaces. As shown in Figure 6a, the −OH and −O− groups from both agar and AAEE can form hydrogen bonds with N, O, and F components of solid materials (e.g., FeN, SiO_2, ZnF) to improve the adhesion, while the C═O and N−H groups from AAEE could offer not only hydrogen bonding with −OH and $-NH_2$ groups of the solid materials but also possible metal complexation with the oxidized metal ions on the solid surface for adhesion. Moreover, van der Waals and hydrophilic interactions could also contribute additional surface adhesion due to close contacts between hydrogel and solid surfaces.

At a first glance in Figure 6b, Agar/pAAEE hydrogels can easily adhere to different solid surfaces like rubber, ceramic, wood, cracker, paper, stainless steel, glass, and aluminum, without any surface modification. To quantitively characterize the adhesive strength of Agar/pAAEE DN gels on solid surfaces, a glass slide was first selected as a model nonporous solid. In Figure 7a, a lap shearing test was used to measure the adhesive energy of Agar/pAAEE DN gels on a nonporous glass at the peeling rate of 5 mm/min, where both sides of the gel were bonded to glass slide, and each side of glass was clamped. By pulling up the upper clamp at a constant crosshead speed of 5 mm/min, the lap shearing test showed a typical shear stress-extension curve, where Agar/pAAEE DN gel achieved high shear force up to ~32.6 N (i.e., a shear strength of 94.5 kPa), which was 10 times higher than that of pAAEE SN gel (9.5 kPa; Figure 7b). The pAAEE SN gel displayed a very low shear stress plateau simply because of the failure of the bulk gel. Low mechanical strength of bulk gels strongly affects interfacial toughness accompany with the low-energy dissipation as reported in literature.[20] We further studied the shearing speed effect on the adhesive strength of Agar/pAAEE DN gels. Actually, the 5 mm/min shearing speed is quite low, which allows the gel–glass interface to relax sufficiently and to minimize energy dissipation resulting from the hysteresis. However, with the increase of shearing speed from 5 to 100 mm/min, the shearing stress of Agar/pAAEE DN gels also increased from 94 to 272 kPa. The adhesion strength of the

DOI: 10.1021/acsapm.8b00232
ACS Appl. Polym. Mater. 2019, 1, 701−713

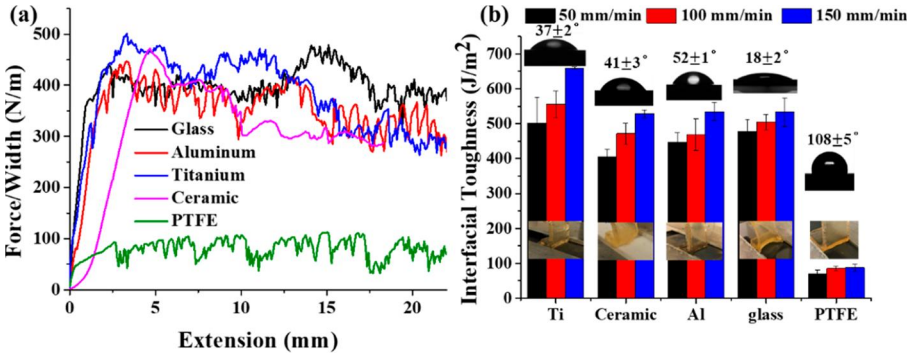

Figure 8. (a) The curves of peeling force per width of Agar/pAAEE DN hydrogel sheet vs displacement at a constant peeling rate of 50 mm/min and (b) interfacial toughness of Agar/pAAEE DN hydrogel on various nonporous solid substrates at different peeling rates and the water contact angles of various nonporous solid substrates.

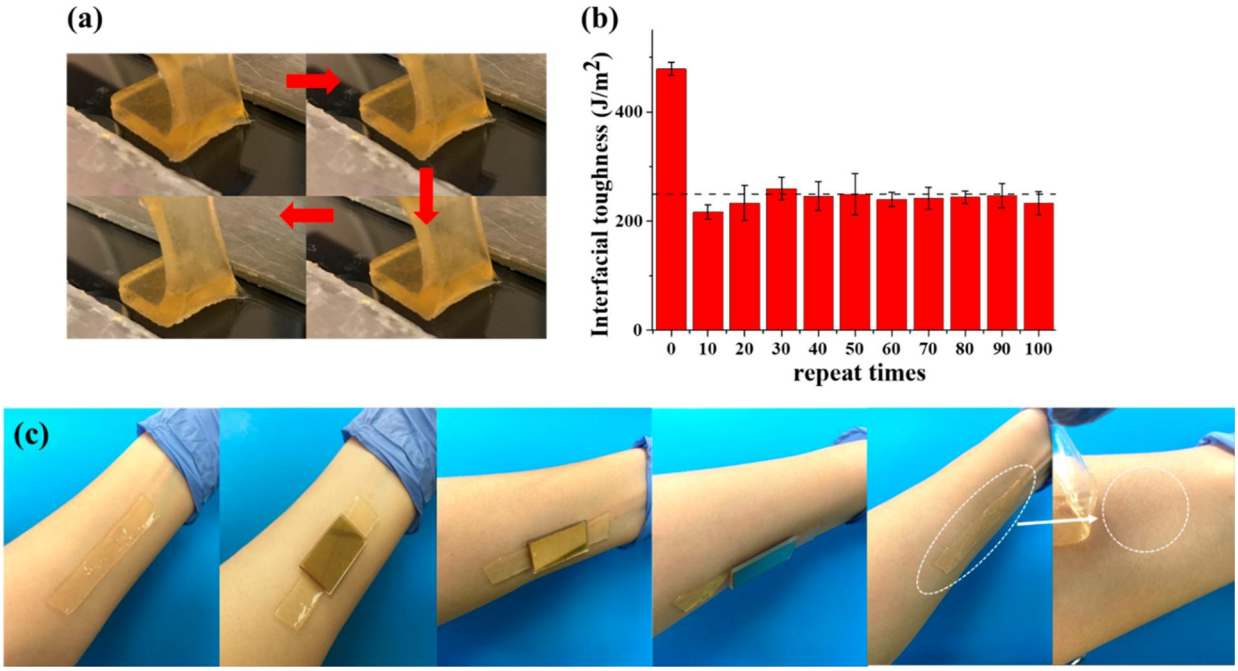

Figure 9. Repeatable surface adhesion of Agar/pAAEE DN hydrogels on a glass, as demonstrated by (a) visual inspection of peeling-off process and (b) average interfacial toughness up to 100 adhesion-on/peel-off cycles. (c) Agar/pAAEE hydrogel serves as an adhesive bridge to directly and steadily adheres on a human arm and a gold chip, and peeling off hydrogel from arm does not cause any residue and pain.

gels is higher than that of the mussel-inspired or dopamine-based hydrogels (~100 kPa under 60 mm/min shearing speed).[39,59,60] The rate-dependent on interfacial toughness is likely attributed to the viscoelasticity of Agar/pAAEE DN gels, which are correlated with the rate-dependent energy dissipation behavior.

More importantly, Agar/pAAEE DN gel has also demonstrated its strong adhesion on different nonporous substrates without any surface modification due to hydrogen bonding-induced physical adhesion (Figure 8). We measured the interfacial toughness of Agar/pAAEE DN gels on different solid surfaces (i.e., glass, aluminum, titanium, ceramics, and poly(tetrafluoroethylene) (PTFE)) using the 90° peeling test at the peeling rate of 50 mm/min. The peeling-force–displacement curves in Figure 8a showed that the measured peeling force of the gels on highly hydrophilic surfaces (glass, aluminum, titanium, and ceramics) was ~300–450 N/m. In a sharp contrast, Agar/pAAEE DN gel weakly adhered on the hydrophobic PTFE surface, with an extremely low peeling force of 50 J/m^2. This result confirms our hypothesis that PTFE surface is too hydrophobic to form hydrogen bonds with Agar/pAAEE DN gel at the PTFE–gel interface. Then, we further examined the effects of peeling rate on the interfacial toughness of Agar/pAAEE DN gels. Interfacial toughness is estimated by the average force per width obtained from the relatively steady-state region in Figure 8a, and the results were presented in Figure 8b. At 50 mm/min peeling rate, the interfacial toughness of Agar/pAAEE DN gels was ~400 J/m^2 on ceramic, ~450 J/m^2 on aluminum, ~480 J/m^2 on glass, and 500 J/m^2 on titanium. Among solid substrates, the adhesive force of the hydrogels on titanium was the highest probably because of the synergistic effects of metal complexation and hydrogen bonding. In contrast, hydrophobic interaction is probably the primary factor in the decreased adhesion of the hydrogels on PTFE, presenting the weakest interfacial toughness (~80 J/m^2). Thus, high interfacial toughness

DOI: 10.1021/acsapm.8b00232
ACS Appl. Polym. Mater. 2019, 1, 701–713

appears to correlate with surface hydrophilicity as indicated by water contact angle. It can be seen in Figure 8b that all the surface presented small contact angles of 20−50°. Moreover, when increasing the peeling rate from 50 to 150 mm/min, the interfacial toughness of Agar/pAAEE DN gels on each solid surface increased monotonously, that is, from 501.2 ± 73.9 to 659.2 ± 2.6 J/m^2 on titanium, from 404.7 ± 22.1 to 528.6 ± 11.1 J/m^2 on ceramics, from 446.5 ± 27.8 to 534.6 ± 26.3 J/m^2 on aluminum, and from 478.7 ± 32.9 to 533.1 ± 40.9 J/m^2 on glass, respectively, all of which are considered as tough adhesive interface. The strong adhesion is attributed to both high bulk toughness and intensive physical interactions between hydrogels and solids. Thus, different physical interactions (hydrogen bonding, metal complexation, van der Waal, and hydrophilic interaction as described above) could lead to different adhesion strength for various solids.

Because of the physical adhesion at the gel−solid interface, it is expected that Agar/pAAEE DN gels could have reversible adhesion capacity on solid surfaces. To directly visualize the adhesive performance of the gel on the glass, Figure 9a showed that, during the peeling process, interfacial bonds between Agar/pAAEE DN gel and a glass were so strong that some fingerlike stripping lag was observed at the gel−substrate interface. The existence of stripping lag demonstrates excellent adhesive behavior, although the gel still can be completely peeled off from the glass and retained intact due to high bulk toughness of the gel itself. Different from chemical anchorage adhesion on surfaces, our Agar/pAAEE hydrogels only involve physical adhesion to the substrate surfaces. Chemical anchorage adhesion often vanishes once chemically bonds are broken at the interface, while physical adhesion could enable reusable and reversible adhesion. To test reversible adhesion behavior, we conducted 100 times of adhesion-on/peel-off cycles for Agar/pAAEE DN gel on the glass. For each cycle, there was no resting time between adhesion-on and peel-off actions; that is, once the gel was peeled off from the glass, it will be immediately reattached on the glass. After every adhesion-on/peel-off cycle, we averaged the interfacial toughness of the gel on the glass. As show in Figure 9b, during the first 90° peeling-off test, the initial interfacial toughness of the as-prepared gel on the glass was as high as ∼480 J/m^2. After that, while the interfacial toughness was dropped to ∼250 J/m^2, it remained almost unchanged even after 100 peel-off/adhesion-on cycles. This indicates that, upon the formation of in situ gel network at gel−solid interface, the interfacial hydrogen bonds between hydroxyl and amide groups of the gel and the silicon dioxides/polar groups of the glass can be reconstructed partially yet sufficiently. Different from those superadhesive hydrogels, where bulk toughness plays an important part in interfacial toughness, the interfacial toughness of Agar/AAEE hydrogels mainly comes from interfacial bondings, not from the recovery of bulk hydrogels. In addition, during the readhere process, some unavoidable bubbles exist at the hydrogel−solid interfaces, which makes it harder to fully recover interfacial bonds and toughness. Both effects explain the decrease of interfacial toughness of the as-prepared and the reattached gel on the glass. However, such partial synergetic interactions still simultaneously exist at the interface between hydrogels and solid substrates, and they are sufficient enough to achieve reversible adhesion on the glass with almost no loss of adhesion strength since then. The reversible adhesion with moderate adhesion strength of 250 J/m^2 could be appropriate for some biomimetic applications, such as tissue adhesions and wound dressing. We also tested the interfacial toughness after immersing the hydrogel−solid samples in water. As a result, interfacial hydrogen bonds were largely destroyed due to hydrogel swelling and water penetration into the hydrogel−solid interfaces. In addition, the hydrogel experienced non-uniform swelling behavior; that is, the part of hydrogels far away from the solid surface exhibited the larger swollen ratios than that of hydrogels near the solid surface, and such mismatch swelling will also reduce the interfacial bonds. Both effects lead to very weak interfacial toughness (data not shown).

As a proof-of-concept, we applied Agar/pAAEE DN gel to adhere to the skin of the author's arm without any pretreatment of the skin (Figure 9c), where a gold chip was attached to the gel as well. The gold chip can steadily adhere on the gel of the arm without falling out when waving and shaking the arm. After that, the gel can be removed easily from the skin without "sticky" residue on the arm. Several authors also did not feel any damage or pain during the multiple-time adhesion-on/peel-off of the gel on/from their arms. We also compared our Agar/pAAEE DN gel with other adhesive hydrogels in literature in terms of bulk toughness, interfacial toughness, and adhesion reversibility. As shown in Figure 10,

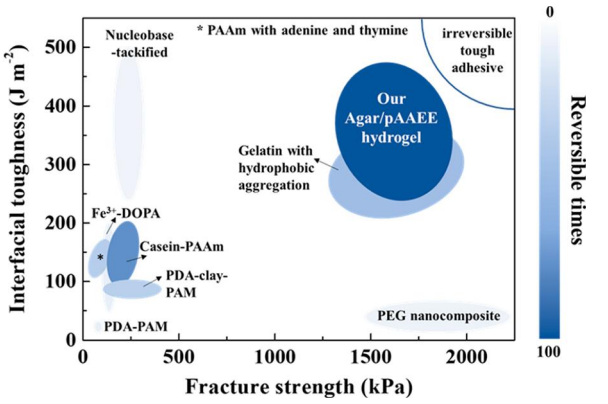

Figure 10. Comparison of bulk toughness, interfacial toughness, and reversibility of Agar/pAAEE hydrogel and other adhesive hydrogels reported in literature.[5,12,14,15,37,39,61]

our Agar/pAAEE DN hydrogel can simultaneously achieve bulk toughness of 1612 J/m^2 and interfacial toughness of ∼650 J/m^2, as well as retain ∼250 J/m^2 of interfacial toughness during 100 cycles, which outperforms other adhesive hydrogels with low bulk toughness, low interfacial toughness, or poor surface adhesion reversibility. Taken together, Agar/pAAEE DN gel has demonstrated the strong and reversible adhesion on both solid and soft surfaces, which outperforms the nonreusable shortcoming of chemical anchorage, expanding for its applications.

4. CONCLUSIONS

In this work, we design and synthesize a fully physically linked DN hydrogel consisting of Agar (the first network)/pAAEE (the second network), where both networks are physically cross-linked via hydrogen bonds. By integrating the reversible physical interactions into the DN network, Agar/pAAEE gel enables to achieve both high bulk toughness and strong, reversible surface adhesion. Bulk Agar/pAAEE hydrogels demonstrate high mechanical properties (tensile stress of

DOI: 10.1021/acsapm.8b00232
ACS Appl. Polym. Mater. 2019, 1, 701−713

1.84 MPa, tensile stain of 2.5 mm/mm, elastic modulus of 1.85 MPa, and tearing energies of 1612 J/m^2) and almost full toughness/stiffness recovery of ~90%/91% after 30 min heating treatment at 80 °C. As supported by its superior bulk mechanical properties, Agar/pAAEE hydrogels can easily and physically adhere on many different solids (glass, titanium, aluminum, and ceramics) and soft surfaces (human skin, muscle tissue) to produce superadhesive hydrogel−surface interfaces (i.e., high interfacial toughness of ~400−650 J/m^2) without any surface modification. More importantly, different from most of one-time-use adhesive hydrogels, Agar/pAAEE hydrogel can be repeatedly adhered on/peeled off on the glass substrate for 100 cycles while still retaining the adhesion strength of ~250 J/m^2, showing repeatable and durable adhesiveness. The gel can also be reversibly adhered on and peeled from human skin, without introducing any hurt. From a structural viewpoint, high mechanical properties and strong/reversible surface adhesion are likely attributed to a combination of physical interactions (hydrogen bonding, metal complexation, and van deer Waal interactions) between and within two networks and between two networks and substrates, as confirmed by swelling behavior, morphological structure, mechanical strength, and adhesive strength. This work demonstrates a new tough gel system with fast, strong, and reversible adhesion on solid and soft surfaces, which will be of great promise and potential for many adhesive-related applications.

■ ASSOCIATED CONTENT

Supporting Information

The Supporting Information is available free of charge on the ACS Publications website at DOI: 10.1021/acsapm.8b00232.

NMR characterizations of AAEE monomer, the effects of both network concentrations on mechanical properties of Agar/pAAEE DN hydrogels (PDF)

■ AUTHOR INFORMATION

Corresponding Authors

*E-mail: xlj235@163.com. (L.X.)
*E-mail: zhengj@uakron.edu. (J.Z.)

ORCID

Ting Wang: 0000-0002-7518-6298
Zhangqi Feng: 0000-0002-1684-588X
Qiang Chen: 0000-0002-8592-9518
Jie Zheng: 0000-0003-1547-3612

Author Contributions

#The authors contributed equally to this work.

Notes

The authors declare no competing financial interest.

■ ACKNOWLEDGMENTS

J.Z. is thankful for financial supports from NSF (DMR-1607475 and CMMI-1825122). We also thank H. Wang (Hangzhou No. 14 High School AP101, China) for her participation and assistance in this project during the summer.

■ REFERENCES

(1) Peppas, N. A.; Hilt, J. Z.; Khademhosseini, A.; Langer, R. Hydrogels in biology and medicine: from molecular principles to bionanotechnology. *Adv. Mater.* **2006**, *18*, 1345−1360.

(2) Lee, K. Y.; Mooney, D. J. Hydrogels for tissue engineering. *Chem. Rev.* **2001**, *101*, 1869−1880.

(3) Li, S.; Jasim, A.; Zhao, W.; Fu, L.; Ullah, M.; Shi, Z.; Yang, G. Fabrication of pH electroactive bacterial cellulose/polyaniline hydrogel for the development of a controlled drug release system. *ES Mater. Manuf.* **2018**, *1*, 41−49.

(4) Heikenfeld, J.; Jajack, A.; Rogers, J.; Gutruf, P.; Tian, L.; Pan, T.; Li, R.; Khine, M.; Kim, J.; Wang, J.; et al. Wearable sensors: modalities, challenges, and prospects. *Lab Chip* **2018**, *18*, 217−248.

(5) Feng, Q.; Wei, K.; Zhang, K.; Yang, B.; Tian, F.; Wang, G.; Bian, L. One-pot solvent exchange preparation of non-swellable, thermoplastic, stretchable and adhesive supramolecular hydrogels based on dual synergistic physical crosslinking. *NPG Asia Mater.* **2018**, *10*, No. e455.

(6) Wei, J.; Wang, J.; Su, S.; Wang, S.; Qiu, J.; Zhang, Z.; Christopher, G.; Ning, F.; Cong, W. 3D printing of an extremely tough hydrogel. *RSC Adv.* **2015**, *5*, 81324−81329.

(7) Rao, P.; Sun, T. L.; Chen, L.; Takahashi, R.; Shinohara, G.; Guo, H.; King, D. R.; Kurokawa, T.; Gong, J. P. Tough Hydrogels with Fast, Strong, and Reversible Underwater Adhesion Based on a Multiscale Design. *Adv. Mater.* **2018**, *30*, 1801884.

(8) Peak, C. W.; Wilker, J. J.; Schmidt, G. A review on tough and sticky hydrogels. *Colloid Polym. Sci.* **2013**, *291*, 2031−2047.

(9) Xiao, S.; Zhang, M.; He, X.; Huang, L.; Zhang, Y.; Ren, B.; Zhong, M.; Chang, Y.; Yang, J.; Zheng, J. Dual Salt- and Thermoresponsive Programmable Bilayer Hydrogel Actuators with Pseudo-Interpenetrating Double-Network Structures. *ACS Appl. Mater. Interfaces* **2018**, *10*, 21642−21653.

(10) Roy, C. K.; Guo, H. L.; Sun, T. L.; Ihsan, A. B.; Kurokawa, T.; Takahata, M.; Nonoyama, T.; Nakajima, T.; Gong, J. P. Self-Adjustable Adhesion of Polyampholyte Hydrogels. *Adv. Mater.* **2015**, *27*, 7344−7348.

(11) Strehin, I.; Nahas, Z.; Arora, K.; Nguyen, T.; Elisseeff, J. A versatile pH sensitive chondroitin sulfate−PEG tissue adhesive and hydrogel. *Biomaterials* **2010**, *31*, 2788−2797.

(12) Han, L.; Yan, L.; Wang, K.; Fang, L.; Zhang, H.; Tang, Y.; Ding, Y.; Weng, L.-T.; Xu, J.; Weng, J.; Liu, Y.; Ren, F.; Lu, X. Tough, self-healable and tissue-adhesive hydrogel with tunable multifunctionality. *NPG Asia Mater.* **2017**, *9*, e372−e372.

(13) Liao, M.; Wan, P.; Wen, J.; Gong, M.; Wu, X.; Wang, Y.; Shi, R.; Zhang, L. Wearable, Healable, and Adhesive Epidermal Sensors Assembled from Mussel-Inspired Conductive Hybrid Hydrogel Framework. *Adv. Funct. Mater.* **2017**, *27*, 1703852.

(14) Kim, B. J.; Oh, D. X.; Kim, S.; Seo, J. H.; Hwang, D. S.; Masic, A.; Han, D. K.; Cha, H. J. Mussel-mimetic protein-based adhesive hydrogel. *Biomacromolecules* **2014**, *15*, 1579−1585.

(15) Xu, J.; Fan, Z.; Duan, L.; Gao, G. A tough, stretchable, and extensively sticky hydrogel driven by milk protein. *Polym. Chem.* **2018**, *9*, 2617−2624.

(16) Amoozgar, Z.; Rickett, T.; Park, J.; Tuchek, C.; Shi, R.; Yeo, Y. Semi-interpenetrating network of polyethylene glycol and photo-crosslinkable chitosan as an in-situ-forming nerve adhesive. *Acta Biomater.* **2012**, *8*, 1849−1858.

(17) Sun, L.; Huang, Y.; Bian, Z.; Petrosino, J.; Fan, Z.; Wang, Y.; Park, K. H.; Yue, T.; Schmidt, M.; Galster, S.; et al. Sundew-inspired adhesive hydrogels combined with adipose-derived stem cells for wound healing. *ACS Appl. Mater. Interfaces* **2016**, *8*, 2423−2434.

(18) Liang, S.; Zhang, Y.; Wang, H.; Xu, Z.; Chen, J.; Bao, R.; Tan, B.; Cui, Y.; Fan, G.; Wang, W.; et al. Paintable and Rapidly Bondable Conductive Hydrogels as Therapeutic Cardiac Patches. *Adv. Mater.* **2018**, *30*, 1704235.

(19) Chen, H.; Liu, Y.; Ren, B.; Zhang, Y.; Ma, J.; Xu, L.; Chen, Q.; Zheng, J. Super Bulk and Interfacial Toughness of Physically Crosslinked Double-Network Hydrogels. *Adv. Funct. Mater.* **2017**, *27*, 1703086.

(20) Yuk, H.; Zhang, T.; Lin, S.; Parada, G. A.; Zhao, X. Tough bonding of hydrogels to diverse non-porous surfaces. *Nat. Mater.* **2016**, *15*, 190−196.

DOI: 10.1021/acsapm.8b00232
ACS Appl. Polym. Mater. 2019, 1, 701−713

(21) Adams, M.; Kerin, A.; Wisnom, M. Sustained loading increases the compressive strength of articular cartilage. *Connect. Tissue Res.* **1998**, *39*, 245−256.
(22) Ambrosio, L.; De Santis, R.; Nicolais, L. Composite hydrogels for implants. *Proc. Inst. Mech. Eng., Part H* **1998**, *212*, 93−99.
(23) Zhao, Y.; Nakajima, T.; Yang, J. J.; Kurokawa, T.; Liu, J.; Lu, J.; Mizumoto, S.; Sugahara, K.; Kitamura, N.; Yasuda, K.; et al. Proteoglycans and Glycosaminoglycans Improve Toughness of Biocompatible Double Network Hydrogels. *Adv. Mater.* **2014**, *26*, 436−442.
(24) Zhao, X. Multi-scale multi-mechanism design of tough hydrogels: building dissipation into stretchy networks. *Soft Matter* **2014**, *10*, 672−687.
(25) Chollet, B.; Li, M.; Martwong, E.; Bresson, B.; Fretigny, C.; Tabeling, P.; Tran, Y. Multiscale surface-attached hydrogel thin films with tailored architecture. *ACS Appl. Mater. Interfaces* **2016**, *8*, 11729−11738.
(26) Zhang, L.; Ma, Y.; Zhao, C.; Zhu, X.; Chen, R.; Yang, W. Synthesis of pH-responsive hydrogel thin films grafted on PCL substrates for protein delivery. *J. Mater. Chem. B* **2015**, *3*, 7673−7681.
(27) Wang, H.; Zha, G.; Du, H.; Gao, L.; Li, X.; Shen, Z.; Zhu, W. Facile fabrication of ultrathin antibacterial hydrogel films via layer-by-layer "click" chemistry. *Polym. Chem.* **2014**, *5*, 6489−6494.
(28) Kharlampieva, E.; Kozlovskaya, V.; Sukhishvili, S. A. Layer-by-Layer Hydrogen-Bonded Polymer Films: From Fundamentals to Applications. *Adv. Mater.* **2009**, *21*, 3053−3065.
(29) Kurokawa, T.; Furukawa, H.; Wang, W.; Tanaka, Y.; Gong, J. P. Formation of a strong hydrogel−porous solid interface via the double-network principle. *Acta Biomater.* **2010**, *6*, 1353−1359.
(30) Saito, J.; Furukawa, H.; Kurokawa, T.; Kuwabara, R.; Kuroda, S.; Hu, J.; Tanaka, Y.; Gong, J. P.; Kitamura, N.; Yasuda, K. Robust bonding and one-step facile synthesis of tough hydrogels with desirable shape by virtue of the double network structure. *Polym. Chem.* **2011**, *2*, 575−580.
(31) Yuk, H.; Zhang, T.; Lin, S.; Parada, G. A.; Zhao, X. Tough bonding of hydrogels to diverse non-porous surfaces. *Nat. Mater.* **2016**, *15*, 190−196.
(32) Wirthl, D.; Pichler, R.; et al. Instant tough bonding of hydrogels for soft machines and electronics. *Sci. Adv.* **2017**, *3*, No. e1700053.
(33) Li, J.; Celiz, A. D.; Yang, J.; Yang, Q.; Wamala, I.; Whyte, W.; Seo, B. R.; Vasilyev, N. V.; Vlassak, J. J.; Suo, Z.; Mooney, D. J. Tough adhesivesfor diverse wet surfaces. *Science* **2017**, *357*, 378−381.
(34) Yang, J.; Bai, R.; Suo, Z. Topological adhesion of wet materials. *Adv. Mater.* **2018**, *30*, 1800671.
(35) Burke, K. A.; Roberts, D. C.; Kaplan, D. L. Silk Fibroin Aqueous-Based Adhesives Inspired by Mussel Adhesive Proteins. *Biomacromolecules* **2016**, *17*, 237−245.
(36) Shin, J.; Lee, J. S.; Lee, C.; Park, H.-J.; Yang, K.; Jin, Y.; Ryu, J. H.; Hong, K. S.; Moon, S.-H.; Chung, H.-M.; Yang, H. S.; Um, S. H.; Oh, J.-W.; Kim, D.-I.; Lee, H.; Cho, S.-W. Tissue Adhesive Catechol-Modified Hyaluronic Acid Hydrogel for Effective, Minimally Invasive Cell Therapy. *Adv. Funct. Mater.* **2015**, *25*, 3814−3824.
(37) Liu, Y.; Meng, H.; Konst, S.; Sarmiento, R.; Rajachar, R.; Lee, B. P. Injectable dopamine-modified poly(ethylene glycol) nanocomposite hydrogel with enhanced adhesive property and bioactivity. *ACS Appl. Mater. Interfaces* **2014**, *6*, 16982−16992.
(38) Wu, H.; Sariola, V.; Zhu, C.; Zhao, J.; Sitti, M.; Bettinger, C. J. Transfer Printing of Metallic Microstructures on Adhesion-Promoting Hydrogel Substrates. *Adv. Mater.* **2015**, *27*, 3398−404.
(39) Han, L.; Lu, X.; Liu, K.; Wang, K.; Fang, L.; Weng, L. T.; Zhang, H.; Tang, Y.; Ren, F.; Zhao, C.; Sun, G.; Liang, R.; Li, Z. Mussel-Inspired Adhesive and Tough Hydrogel Based on Nanoclay Confined Dopamine Polymerization. *ACS Nano* **2017**, *11*, 2561−2574.
(40) Kim, D.-H.; Lu, N.; Huang, Y.; Rogers, J. A. Materials for stretchable electronics in bioinspired and biointegrated devices. *MRS Bull.* **2012**, *37*, 226−235.
(41) Liu, X.; Zhang, Q.; Gao, Z.; Hou, R.; Gao, G. Bioinspired Adhesive Hydrogel Driven by Adenine and Thymine. *ACS Appl. Mater. Interfaces* **2017**, *9*, 17645−17652.
(42) Chen, H.; Liu, Y.; Ren, B.; Ma, J.; Xu, L.; Chen, Q.; Zheng, J.; et al. Super bulk and interfacial toughness of physically-crosslinked double-network hydrogels. *Adv. Funct. Mater.* **2017**, *27*, 1703086.
(43) Chen, H.; Zhang, M.; Yang, J.; Zhao, C.; Hu, R.; Chen, Q.; Chang, Y.; Zheng, J. Synthesis and characterization of antifouling poly(N-acryloylaminoethoxyethanol) with ultralow protein adsorption and cell attachment. *Langmuir* **2014**, *30*, 10398−10409.
(44) Chen, Q.; Zhu, L.; Zhao, C.; Wang, Q.; Zheng, J. A robust, one-pot synthesis of highly mechanical and recoverable double network hydrogels using thermoreversible sol-gel polysaccharide. *Adv. Mater.* **2013**, *25*, 4171−4176.
(45) Greensmith, H. W.; Thomas, A. G. Rupture of rubber. III. Determination of tear properties. *J. Polym. Sci.* **1955**, *18*, 189−200.
(46) Chiari, M.; Micheletti, C.; Nesi, M.; Fazio, M.; Righetti, P. G. Towards new formulations for polyacrylamide matrices: N-acryloylaminoethoxyethanol, a novel monomer combining high hydrophilicity with extreme hydrolytic stability. *Electrophoresis* **1994**, *15*, 177−186.
(47) Chen, Q.; Zhu, L.; Chen, H.; Yan, H.; Huang, L.; Yang, J.; Zheng, J. A novel design strategy for fully physically linked double network hydrogels with tough, fatigue resistant, and self-healing properties. *Adv. Funct. Mater.* **2015**, *25*, 1598−1607.
(48) Chen, H.; Yang, F.; Hu, R.; Zhang, M.; Ren, B.; Gong, X.; Ma, J.; Jiang, B.; Chen, Q.; Zheng, J. A comparative study of the mechanical properties of hybrid double-network hydrogels in swollen and as-prepared states. *J. Mater. Chem. B* **2016**, *4*, 5814−5824.
(49) Samiey, B.; Ashoori, F. Adsorptive removal of methylene blue by agar: effects of NaCl and ethanol. *Chem. Cent. J.* **2012**, *6*, 14.
(50) Sudre, G.; Olanier, L.; Tran, Y.; Hourdet, D.; Creton, C. Reversible adhesion between a hydrogel and a polymer brush. *Soft Matter* **2012**, *8*, 8184−8193.
(51) Gong, J. P.; et al. Double-Network hydrogels with extremely high mechanical strength. *Adv. Mater.* **2003**, *15*, 1155−1158.
(52) Chen, H.; Zhao, C.; Zhang, M.; Chen, Q.; Ma, J.; Zheng, J. Molecular Understanding and Structural-Based Design of Polyacrylamides and Polyacrylates as Antifouling Materials. *Langmuir* **2016**, *32*, 3315−3330.
(53) Kwon, H. J.; Rogalsky, A. D.; Kim, D.-W. On the measurement of fracture toughness of soft biogel. *Polym. Eng. Sci.* **2011**, *51*, 1078−1086.
(54) Chen, Q.; Wei, D.; Chen, H.; Zhu, L.; Jiao, C.; Liu, G.; Huang, L.; Yang, J.; Wang, L.; Zheng, J. Simultaneous enhancement of stiffness and toughness in hybrid double-network hydrogels via the first, physically linked network. *Macromolecules* **2015**, *48*, 8003−8010.
(55) Mao, Y.; Lin, S.; Zhao, X.; Anand, L. A large deformation viscoelastic model for double-network hydrogels. *J. Mech. Phys. Solids* **2017**, *100*, 103−130.
(56) Sun, J.-Y.; Zhao, X.; Illeperuma, W. R.; Chaudhuri, O.; Oh, K. H.; Mooney, D. J.; Vlassak, J. J.; Suo, Z. Highly stretchable and tough hydrogels. *Nature* **2012**, *489*, 133−136.
(57) Sun, T. L.; Kurokawa, T.; Kuroda, S.; Ihsan, A. B.; Akasaki, T.; Sato, K.; Haque, M. A.; Nakajima, T.; Gong, J. P. Physical hydrogels composed of polyampholytes demonstrate high toughness and viscoelasticity. *Nat. Mater.* **2013**, *12*, 932−937.
(58) Chen, Q.; Chen, H.; Zhu, L.; Zheng, J. Fundamentals of double network hydrogels. *J. Mater. Chem. B* **2015**, *3*, 3654−3676.
(59) Shan, M.; Gong, C.; Li, B.; Wu, G. A pH, glucose, and dopamine triple-responsive, self-healable adhesive hydrogel formed by phenylborate−catechol complexation. *Polym. Chem.* **2017**, *8*, 2997−3005.
(60) Guvendiren, M.; Messersmith, P. B.; Shull, K. R. Self-assembly and adhesion of DOPA-modified methacrylic triblock hydrogels. *Biomacromolecules* **2008**, *9*, 122−128.
(61) Liu, X.; Zhang, Q.; Gao, G. Bioinspired Adhesive Hydrogels Tackified by Nucleobases. *Adv. Funct. Mater.* **2017**, *27*, 1703132.

DOI: 10.1021/acsapm.8b00232
ACS Appl. Polym. Mater. 2019, 1, 701−713